



SEISMIC VULNERABILITY EVALUATION OF PERUVIAN AERIAL ELECTRICAL SUBSTATIONS WITH SIMULATED FRAGILITY FUNCTIONS

J. Ruiz⁽¹⁾, M. Rojas⁽²⁾

⁽¹⁾ Mg. Eng., Pontifical Catholic University of Peru, joruize@pucp.pe

⁽²⁾ Lecturer, Engineering National University, macgriver.rr@gmail.com

...

Abstract

This research uses a probabilistic methodology to evaluate the seismic vulnerability of aerial electrical substations in Perú. Peruvian electrical distribution substations are vital structures for which exists little research about their seismic vulnerability. This paper aims to be a contribution to estimate the seismic vulnerability of vital electrification lines. The proposed methodology is based on fragility functions which represent the overall structural behavior of 3D model frames for 27 aerial distribution electrical substations located in Cañete city.

The Latin Hypercube technique, an enhanced Monte Carlo-base method, was used to generate fragility functions. This technique optimizes the sampling of structural parameters and provides at least 100 reliable samples for every level of seismic demand. In case of structural models, only the concrete compressive strength (f'_c), the maximum concrete strain (ϵ_{cu}) and the yield stress of the reinforcing steel (f_y) were considered. For the concrete, mean values of 20 MPa and 0.40% were considered for compressive strength and maximum strain, respectively. For both cases, 15% coefficient of variation with a normal probability distribution function was assumed. However, for the steel, it was assumed an average value of 412 MPa, a 6.0% coefficient of variation and a lognormal probability distribution function. This is due to higher quality requirements during its fabrication. Axial force was shown to have a direct impact on curvature ductility of reinforced concrete cross sections. The seismic demand was defined by synthetic records that were compatible with the elastic Peruvian design spectrum, considering two soil types (S_1 and S_2) described in Peruvian seismic code. Acceleration records were scaled based on the peak ground acceleration on rigid soil (PGA) which went from 0.05g to 1.00g. A total of 2000 structural models were considered to account for both structural and seismic variability, for each soil type and aerial distribution electrical substation category.

The structural models use frame elements with concentrated plastic flexure hinges. This way, the strength and stiffness degradation of the structure persists overtime. Nonlinear time-history analysis was carried out for each model subjected to a synthetic signal. This was performed with SAP 2000 program. These samples were run without user interaction through MATLAB scripts. The coupling between structural models and signals was performed with Monte Carlo simulation.

On one hand, seismic vulnerability ratios for aerial electrical substations, constructed on S_1 soil type, showed expected average probabilities of 99% and 88% for simple and double post substations respectively, considering a damage limit state as yielding. For the same substations, 1% and 3% ratios were computed for collapse limit state. On the other hand, considering S_2 soil type, ratios showed average probabilities of 86% and 66% in yielding limit state, and 1% ratio was computed for collapse limit in both post type cases. These ratios were computed considering a seismic demand related to 10% of probability of exceedance in 50 years, which is a requirement in the Peruvian seismic code. These results show an unacceptable seismic performance for substations. They may require extensive repairing or complete post reposition.

Keywords: Seismic Vulnerability, Fragility Curves, Monte Carlo simulation, Aerial Electrical Substations.



1. Introduction

The western edge of South America is characterized as one of the most seismically active regions in the world. Peru is part of this region and its most important seismic activity is associated with subduction process of oceanic plate under continental plate, generating high magnitude earthquakes with relative frequency. During the last 50 years, Peru has presented a long seismic which means next earthquake will cause severe structural damage due to the huge amount of accumulated energy. One example was Pisco earthquake on August 15, 2007 which represents one of the most catastrophic seismic events suffered in Peru in recent decades, both for the number of deaths and injuries and for the damage caused to buildings, infrastructure and other structures. The earthquake caused the disconnection of six principal Electrical Substations which interrupted electrical service and affected several cities such as Cañete, Chinchá, Pisco, Ica, Nazca, Huancavelica and its surrounding towns. Aerial distribution electrical substations suffered extensive damage due to the collapse of a significant number of posts, cables and insulators, and public lighting was initially restricted by 95% throughout the region. The absence of electric service lasted several days in some locations, which affected essential services like hospitals, medical establishments and other basic services, such as communication systems, water supply, commerce, fuel sales and banks [1]. Electrical transmission lines inspection and repairing took between three to ten days, depending on damage and localizations according to Peruvian Ministry of Energy and Mines.

This study focuses on the analysis of 27 aerial distribution electrical substations located in Cañete city. Cañete is located in the highest seismic zone according to Peruvian design code, being affected by Pisco earthquake in 2007. This investigation aims to develop fragility functions for seismic vulnerability evaluation of aerial distribution electrical substations. Fragility functions give the probability of exceedance for a given damage state and an Intensity Measure (IM). This work considers a simulation-based analytical method in order to generate fragility functions because of the lack after-earthquake information in Peru. Fragility functions consider uncertainties in structural capacity and seismic demand. Variability of structural capacity is taken by three parameters: the compressive concrete strength (f'_c), the ultimate concrete strain (ϵ_{cu}) and the yielding stress of the reinforcement (f_y). Variability of seismic demand is considered by artificial accelerograms which were generated based on the elastic Peruvian design spectrum. A total of 2000 analyzed models were generated for each aerial distribution electrical substations with different structural capacity and each one was subjected to a different seismic demand with a certain variation of the peak ground acceleration (PGA).

2. Aerial Distribution Electrical Substations in Cañete

A general substation is defined as a set of facilities, including any buildings required to house them, intended for electrical voltage transformation and electrical circuits sectioning and protection, according to Peruvian Ministry of Energy and Mines. The distribution substation is a set of facilities for electrical energy transformation or sectioning received from a primary distribution network that will be delivered to a secondary distribution network, to public lighting installations, to another primary distribution network or directly to users. Aerial distribution electrical substation has an equipment exposed to outside and it classifies in two types: single post distribution substation (SPDS), which has a post that supports an electrical distribution transformer; and double post distribution substation (DPDS), in which two posts are joined by a platform that supports an electrical distribution transformer as shown in Fig.1. This study analyzed 27 aerial distribution electrical substations with different post types. Poles are generally made of reinforced concrete and its design and fabrication are regulated by Peruvian government through INDECOPI [2] and Ministry of Energy and Mines. Additional guidelines about geometric requirements are indicated by *Luz del Sur*, which is a Peruvian regulatory entity that provides different norms that regulate construction of electrical substations.



Fig. 1 – SPDS (left) and DPDS (right)

2.1 Centrifuged post (CP) and support platform (SP)

Reinforced concrete posts are made of a mixture of cement, coarse and fine aggregates, water and additives. A reinforcing steel is placed inside the post to give flexural strength. It is necessary to place the mixture in special molds and it is compacted by mechanical centrifugation and subdued to steam curation. Because of mechanical process, posts adopt a hollow truncated cone shape and internal space is used as housing of electric conductors. Table 1 resumes material and structural properties for a typical 13m CP. According to *Luz del Sur* [3] requirements, distribution of typical reinforcing steel is shown in Fig.2 for different sections along to CP. Longitudinal reinforcement is formed by 12mm rebars whose quantity varies from bottom to top section, being the bottom section the only part that presents 3/8" reinforcement bars that give more flexural strength. Shear reinforcement is defined by 1/4" stirrups which are spaced with a 500 mm step, and all stirrup must be tie and assured with N°16 wire.

Table 1 – 13m CP technical specifications

Material	Description	Value
Concrete	Compressive concrete strength	35 MPa
	Minimum covering thickness	20 mm
Steel	Yielding stress of the reinforcement	420 MPa
	Minimum stirrup size	Φ1/4"
	Minimum longitudinal reinforcement	Φ 12 mm or Φ1/4"



Fig. 2 – Typical 13m length CP (left) and its reinforcing steel distribution (right)



Support platforms are made by same materials and constructive process as shown in Fig.3, and they support distribution transformers. A half SP is used in SPDS and two half SP are used in DPDS. The power of the distribution transformer defines SP weight and it is possible to distinguish two different types: 1500 kg and 2600 kg.

2.2 Double *palomilla* (DP), bracket (BK) and symmetric or asymmetric crosshead (SC/AC)

These three components are made of reinforced concrete and its fabrication process follow same guidelines as CRCP and SP, but only AC are made of wood. DP supports disconnecting fuses (cut out) and its dimensions and weight depend on the power of the distribution transformer: 60 kg for 250 kVA and 100 kg for 630 kVA. Brackets and crossheads are used for PIN type installation or they function as suspension insulators in aerial medium voltage lines such as 10 kV and 22.9 kV.



Fig. 3 – Typical SP (a), DP (b), BK (c) and SC/AC (d)

2.3 Distribution transformers (DT)

DT are the most important electrical elements in aerial distribution electrical substation and its installed power allows to select SP and DP types. Fig.4 and Table 2 indicate DT powers, dimensions and weights for a 10kV voltage level. DT weight is an important force to define in posts structural analysis.

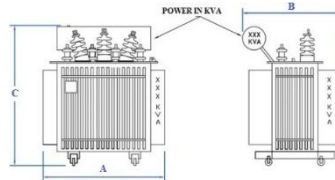


Fig. 4 – DT sizing for a 10 kV voltage level

Table 2 – Typical power, dimensions and weight of DT

Power (kVA)	Maximum dimensions (mm)			Weight (kgf)
	A	B	C	
50	850	660	1300	315
100	950	690	1400	515
160	1050	780	1530	710
250	1250	850	1600	1030
400	1380	1000	1650	1460

2.4 Specific data summary

Materials and structural properties of SP, DP, BK and SC/AC are resumed in Table 3. Additional guidelines are considered in *Luz del Sur* norms [4, 5, 6, 7, 8, 9, 10].



Table 3 – Typical materials and structural properties of SP, DP, BK and SC/AC

Material	Description	Value
Concrete	Compressive concrete strength	28 MPa
	Minimum covering thickness	15 mm
Steel	Yielding stress of the reinforcement	420 MPa
	Minimum stirrup size	Φ1/4"
	Minimum longitudinal reinforcement	Φ3/8"

Table 4 resumes some specific data of the 27 aerial distribution electrical substations collected on field and describes the following parameters: structural and functional typology, reinforced concrete components (C), wooden parts (M), pole height, power of the transformer and electrical voltage level.

Table 4 – Aerial distribution electrical substations

Item	Structural Type	CP	SP	DP	BK	SC	AC	Height (m)	Power (kVA)	Voltage (kV)
01	DPDS	C	C	C	---	C	---	13	250	10
02	DPDS	C	C	C	---	---	M	13	250	10
03	DPDS	C	C	C	---	---	M	13	400	10
04	SPDS	C	C	---	---	---	M	13	100	10
05	DPDS	C	C	C	---	---	M	13	250	10

3. Seismic hazard in Cañete city

To estimate seismic demand in Cañete city, it was necessary to carry out a Probabilistic Seismic Hazard Assessment (PSHA) based on SENCICO Seismic Hazard Consultation Web Site [11, 12] which gives next information: annual exceedance probability curves versus spectral acceleration, uniform hazard spectra and seismic design spectra determined considering Peruvian seismic code [13]. Input data is required as follows: latitude and longitude of emplacement, structural period and damping structure. In this study it was considered Cañete location, a structural period of 0 seconds because it represented PGA, and damping was considered as 5% for reinforced concrete structures (posts). After introducing initial data, SENCICO Web Site estimates seismic hazard curve that represents relationship between spectral acceleration and exceedance annual probability. According to Peruvian seismic code, seismic demand related to 10% probability of exceedance in 50 years means a return period of 475 years. Annual exceedance probability for this return period is calculated as its inverse resulting in 0.0021. This value is projected on seismic hazard curve obtaining a PGA of 0.475g for Cañete city as shown in Fig.5.

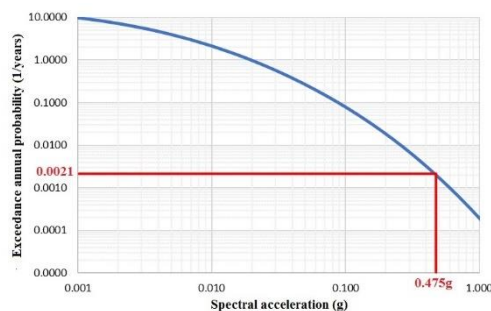


Fig. 5 – Probabilistic seismic hazard curve for Cañete city



4. Monte Carlo simulation

Monte Carlo simulation is a technique used to model the probability of different outcomes of physical systems, in a process that cannot easily be predicted due to the intervention of random variables. Probability density function are the main input data in this process. Although posts were built under similar conditions, there will be the probability of having different mechanical properties, and this will affect structural behavior. Simulation process permits to consider this variation on structural analysis.

4.1 Uncertainty in the structural parameters

Structural variability was considered by taking three parameters inside simulation process: the concrete compression strength (f'_c), the ultimate concrete strain (ϵ_{cu}) and the yielding stress of the reinforcing steel (f_y). Ruiz [14] proposes average values for experimental data and suggests next ones: f'_c and ϵ_{cu} could take a 15% coefficient of variation for a normal probability density function and average values of 21 MPa and 0.004 (Hognestad model) respectively, and for f_y suggests a 6% coefficient of variation and an average value of 420 MPa. Sampling procedure was generated by using Latin Hypercube technique which is an improved Monte Carlo simulation process. Fig.6 shows probability density functions which are necessary to define 100 random samples with different structural parameters for each IM. Functions were made with MATLAB [15] scripts.

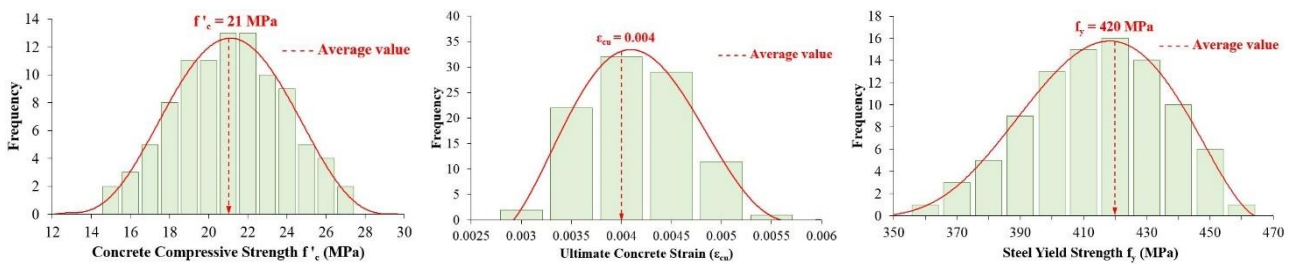


Fig. 6 – Probability density functions for structural parameters

4.2 Uncertainty in seismic parameters

Artificial records were used to model seismic action in Nonlinear Time History Analysis (NTHA). These signals are used due to the lack of recent earthquakes records. Signals were scaled to the elastic response design spectrum detailed in the Peruvian seismic code and a wide range of seismic intensity to incite a inelastic structural post behavior was considered. It was necessary to use periodic functions, which are based on acceleration $\ddot{u}_g(t)$, to generate compatible artificial accelerograms. This seismic function is expressed as series of sinusoidal waves according to Eq. (1).

$$\ddot{u}_g(t) = \sum_{k=1}^n A_k \text{sen}(w_k t + \phi_k) \quad (1)$$

Where A_k is the amplitude, w_k is the angular frequency and ϕ_k is the phase angle of the k sinusoidal contribution. It was necessary to insert a function named $I(t)$ (intensity envelope) inside Eq. (1) in order to simulate the transient behavior of real accelerograms. Final equation is given by Eq. (2).

$$\ddot{u}_g(t) = I(t) \sum_{k=1}^n A_k \text{sen}(w_k t + \phi_k) \quad (2)$$

This study chose trapezoidal intensity function because it represents a simple and better adjudgment for Peruvian artificial signals. According to Moreno [16] and using Pisco earthquake parameters as representative real accelerogram that generated damage at Cañete in 2007, the intensity function was defined with 42 seconds of total duration which considers 15 seconds of rising time (t_s) and 39 seconds of strong motion (t_f).



In order to define the amplitude, it was important to create Peruvian elastic design spectrums considering two kinds of soils: S_1 (rock or very rigid soils) and S_2 (intermediate soils) which are defined in Peruvian seismic code and verified on Cañete soil typologies as shown in Fig.7.

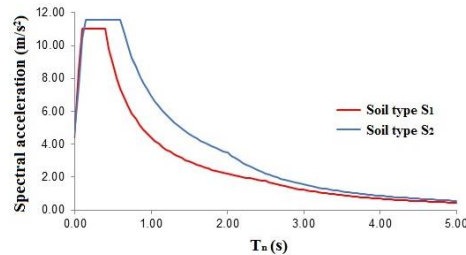


Fig. 7 – Elastic design spectrum for soil type S_1 and S_2 for a 0.45g PGA

SeismoArtif [17] software was used to generate artificial signals through an artificial generation method, which needs two principal input data: a spectrum curve and an intensity function. Random synthetic records were produced considering phase angle variation from 0 to 2π . Signals were also compatible to the uniform hazard spectrum proposed by the Peruvian seismic design code and their PGA values varied from 0.05g to 1.00g with 0.05g increases. Fig.8 shows two artificial accelerograms that were generated for S_1 and S_2 soil types respectively, considering a PGA of 0.50g. In addition, Fig.9 shows compatibility between the artificial signal spectrums, described previously, and elastic seismic design code.

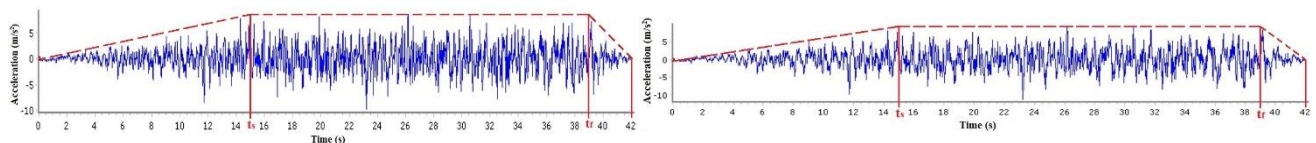


Fig. 8 – Artificial signals scaled up to a PGA of 0.50g considering S_1 (left) and S_2 (right) soil types

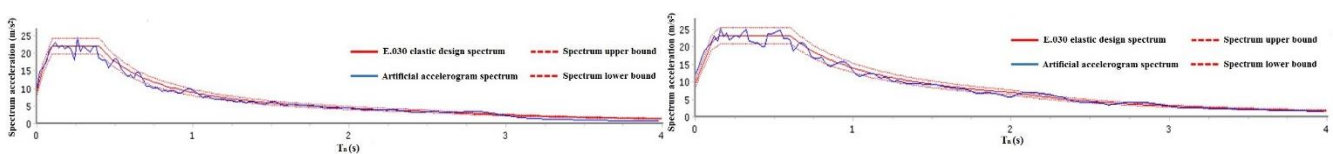


Fig. 9 – Scaled artificial accelerograms spectrums and its corresponding E.030 elastic compatible design spectrum considering S_1 (left) and S_2 (right) soil types

4. Nonlinear time history analysis (NTHA)

SAP2000 [18] permitted to model and analyze a random population of 3D frames generated with the Latin Hypercube technique, which is an improved Monte Carlo method. Concentrated plastic hinges were modeled considering nonlinear material properties. Paulay and Priestley [19] recommended assigned plastic hinges at an equivalent length (L_p) of $0.5h$, where h represents overall depth of the structural element cross section parallel to analyzed direction. Considering an equivalent plastic length of constant curvature, rotation can be determined by multiplying the length and curvature. Constitutive laws of materials and their hysteretic relationships were used to create plastic hinges. A perfect elastoplastic behavior was taken for reinforcing steel. Hognestad model for unconfined concrete was assumed to concrete cross section. Material constitutive laws are shown in Fig.10.

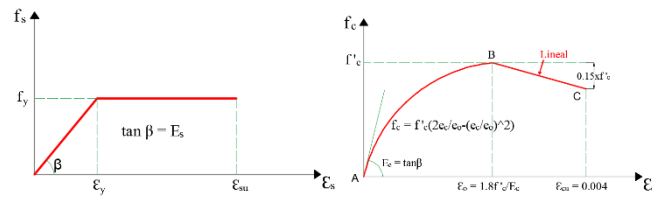


Fig. 10 – Perfect elastoplastic function for reinforcing steel (left) and Hognestad model for unconfined concrete (right)

Moment-curvature diagrams allows to consider inelastic deformation capacity of a structural element. This study considered a section transformation from hollow to rectangular shape considering equality of cross section area and preserving overall diameter of hollow shape as overall depth of rectangular form. Eq. (3) and Eq. (4) show general transformation process.

$$h = D_e \quad (3)$$

$$b = \frac{\pi}{4} \left(\frac{D_e^2 - D_i^2}{D_e} \right) \quad (4)$$

Where h is the overall depth of rectangular section, D_e and D_i are the overall and interior diameters of hollow shape respectively, and b is the rectangular base section. Three different section types were identified for reinforcing steel distribution: a bottom section that presents $9\Phi 12\text{mm}$ and $3\Phi 3/8''$, an intermediate section that contains $9\Phi 12\text{mm}$ and a top section with $6\Phi 12\text{mm}$, as shown in Fig.11. In all cases, reinforcing steel was considered from compression edge (top) of the transformed shape to the center of reinforcing steel bar.

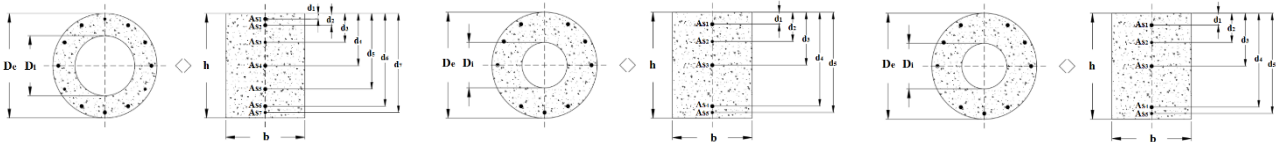


Fig. 11 – Original hollow shapes and bottom rectangular transformed shapes for bottom section (left), intermediate section (middle) and top section (right)

Moment-curvature column diagrams are highly influenced by axial force levels, this study took the second load combination of the Peruvian concrete design code [20] (i.e. $1.25 \text{ DL} + 1.25 \text{ LL}$) for moment-curvature relationship for this structural element during the NTHA. Fig.12 shows typical moment-curvature relationships for SPDS and DPDS.

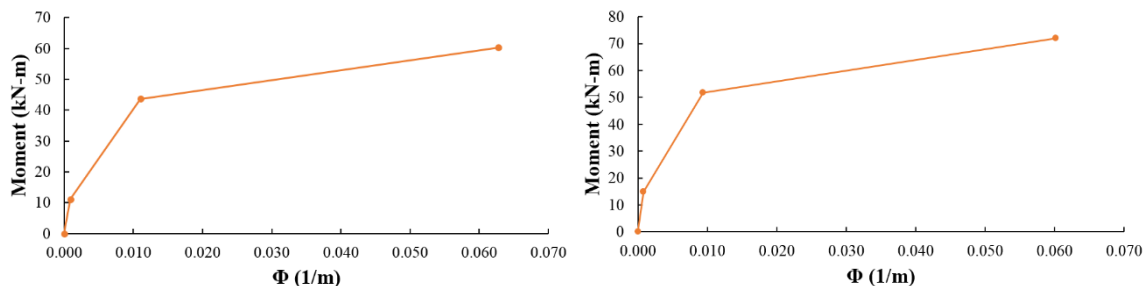


Fig. 12 – Moment-curvature diagrams for SPDS bottom section (left) and DPDS bottom section (right)



A primary curve is defined by moment-curvature diagram and hysteresis behavior was defined by Takeda et. al. [21] model. This model is considered appropriate for concrete structural elements when energy dissipation and bending-compression behavior is required. With the previous information and creating algorithms in MATLAB, it was possible to analyze a total of 2000 random structural models for each of the 27 aerial distribution electrical substations without user interaction.

5. Fragility functions and seismic vulnerability

5.1 Damage limit states

Pushover analysis is a static nonlinear analysis which permit us to define Damage Limit States (DLS) for a specific structure. This analysis obtains a Capacity Curve of structure through a series of incremental static nonlinear analysis. Constitutive material models and hysteresis relationships defined before are important information to define Capacity Curve. This curve can be elaborated by using first mode response (fundamental mode) which is considered as the most relevant deformed state in structural analysis. Curve construction method consists in recording the top displacement of structure and the base shear while lateral load increases. This process ends when maximum lateral displacement capacity is achieved [22]. In order to simplify capacity curve, it is necessary to build a simplified trilinear model following Aguilar [23] guidelines. This procedure recommends to reach equivalent inside and outside areas throughout a trilinear model. This work selected first the mode lateral load pattern which is easily defined in SAP2000.

At present exists guidelines that permit to define DLS and Seismic Performance Levels (SPL) for building such as VISION 2000 or ATC-40 committees. However, there is little or almost no information about these topics for other structures like reservoirs, retaining walls, electrical substation and so on. For that reason, this study proposes four DLS and its corresponding SPL, following INEN [24, 25] guidelines which is an Ecuadorian code that regulates reinforced concrete posts building. Table 5 resumes DLS and SPL that were applied for post seismic vulnerability.

Table 5 – DLS and SPL according to INEN [24, 25]





DLS (Proposed)	Damage Description	SPL (Proposed)	Main Characteristics	Pictures
LS1: Initial Cracking	Posts must not present concrete covering spalling in compression edge nor cracks opening greater than 0.05 mm in tension edge. Top displacement is determined for 20% of nominal failure load.	Operational	Light structural damage. Electric distribution service is operational. No repairs.	
LS2: Cracking Opening	Posts must not present concrete covering spalling in compression edge nor cracks opening greater than 0.10 mm in tension edge. Top displacement is determined for 30% of nominal failure load.	Functional	Moderate structural damage. All electricity distribution services are still functioning. Few repairs.	
LS3: Yielding	Concrete covering spalling exists in partial or entire section, and steel reinforcing bars work under compression and traction stresses due to cyclic lateral forces. Reinforcing bars reach yielding stress and they lengthen. Aguilar [23] guidelines define yielding displacement in capacity curves.	Pre collapse	Severe structural damage. Stiffness degradation and resistance loss compromise structure stability. Partial interruption occurs in electricity distribution services. Repairs can be unfeasible.	
LS4: Collapse	Structural strength is overcome and immediate failure occurs. Reinforcing steel stresses exceed maximum failure stress	Collapse	Complete structural damage. Total electricity distribution service interruption. Collapse area is insecure for population.	

Table 6 presents damage limit state values for SPDS and DPDS considering critical maximum interstory drift ratio between X and Y directions. Fig.13 shows capacity curves for SPDS and DPDS, and their corresponding damage limit states.



Table 6 – Damage limit state values for SPDS and DPDS

DLS	SPDS			DPDS		
	Top Displacement (m)	Base Shear (kN)	Max. Interstory Drift ratio	Top Displacement (m)	Base Shear (kN)	Max. Interstory Drift ratio
LS1	0.059	2.10	0.50%	0.053	4.39	0.45%
LS2	0.084	3.15	0.71%	0.078	6.59	0.66%
LS3	0.182	7.35	1.56%	0.181	15.71	1.55%
LS4	0.348	10.50	2.98%	0.344	21.96	2.94%

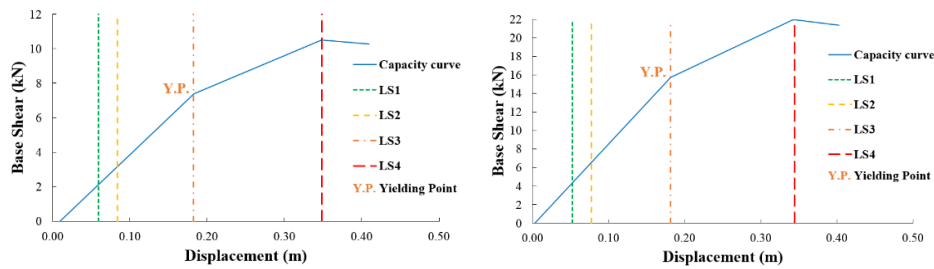


Fig. 12 – Capacity curves for a SPDS (left) and a DPDS (right)

5.2 Damage probability density function

The function $f(x)$ was defined as the probability density function of a random continuous variable. It is necessary to integrate this function in the interval $[a, b]$ to represent the probability of occurrence for real values between a and b . Eq. (5) shows this definition.

$$P[a \leq x \leq b] = \int_a^b f(x) dx \quad (5)$$

When integration limits vary between $-\infty$ and x , a new function appears which is known as cumulative probability density function $F_X(x_i)$ (CDF). Results were sorting in ascending order applying Eq. (6). x_i is the event that may repeat i times inside a population with $n(S)$ sample size. When CDF is computed over entire real domain, Eq. (7) is obtained and it means that the probability of being less than infinite is 1 and the complementary event defined as the Probability of Exceedance can be calculated by Eq. (8). This probability of exceedance represents the limit value of damage limit states and permits to plot fragility functions.

$$F_X(x_i) = \frac{i}{n(S)} \quad (6)$$

$$\int_{-\infty}^{\infty} f(x) dx = F_X(\infty) = \lim_{x \rightarrow +\infty} F(x) = 1 \quad (7)$$

$$P[X > x] = 1 - F_X(x) \quad (8)$$

5.3 Probability of exceedance, fragility functions and seismic vulnerability

The probability of exceedance of a specific DLS is determined by fragility functions given an IM. IM was defined as PGA and pseudo-acceleration (S_a). Fragility function generation methods adjust values into a lognormal probability density functions (ϕ) (LPDF) defined by Eq. (9).



$$P(DLS \geq DLS_i/IM) = \phi \left[\frac{1}{\beta_{IM,DLS_i}} \ln \left(\frac{IM}{\overline{IM}} \right) \right] \quad (8)$$

Where \overline{IM} represents the average value of IM for DLS_i . β_{IM,DLS_i} denotes coefficient of variation for the DLS_i , and ϕ is the LPDF. With MATLAB scripts, fragility functions were built for the 27 aerial distribution electrical substations. Fig. 13 shows some fragility functions for SPDS and DPDS.

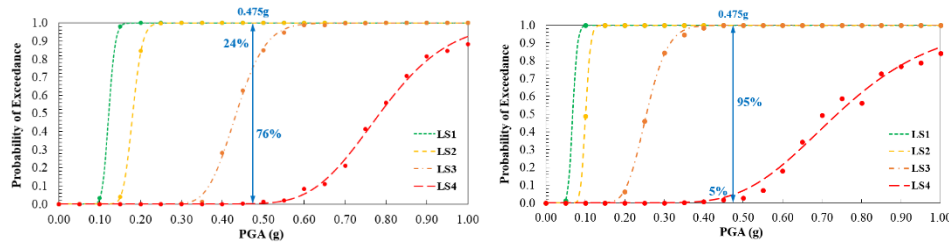


Fig. 13 – Simulated fragility functions for a SPDS (left) and a DPDS (right) in terms of PGA

Seismic vulnerability was obtained from simulated fragility functions, which represent probability of exceedance of a DLS. PSHA determined a PGA of 0.475g as hazard scenario which will determine probability of exceedance for the 27 aerial distribution electrical substations as shown in Table 7 and Table 8.

Table 7 – Seismic vulnerability ratios of 14 aerial distribution electrical substation in terms of a 0.475g PGA

Seismic Vulnerability	DLS	0012	0013	0015	0016	0408	0011	0009	0628	0726	0378	0018	0017	0019	0020
		DPDS	DPDS	DPDS	SPDS	DPDS	DPDS	DPDS	SPDS	SPDS	SPDS	DPDS	DPDS	DPDS	DPDS
	S ₁	S ₁	S ₁	S ₁	S ₁	S ₁	S ₁	S ₁	S ₁	S ₁	S ₁	S ₁	S ₂	S ₂	S ₁
	LS1	0%	0%	0%	0%	0%	0%	0%	0%	0%	0%	0%	0%	0%	0%
LS2	33%	34%	20%	9%	27%	33%	30%	9%	9%	15%	35%	15%	0%	35%	
LS3	67%	64%	79%	90%	72%	67%	68%	90%	90%	84%	64%	82%	99%	64%	
LS4	0%	2%	1%	1%	1%	0%	2%	1%	1%	1%	1%	3%	1%	0%	

Table 8 – Seismic vulnerability ratios of 13 aerial distribution electrical substation in terms of a 0.475g PGA

Seismic Vulnerability	DLS	0648	0024	0023	0022	0021	0803	0496	0097	0662	0700	0689	0405	0647
		SPDS	DPDS	DPDS	DPDS	DPDS	SPDS	SPDS	DPDS	SPDS	SPDS	SPDS	DPDS	SPDS
	S ₂	S ₂	S ₂	S ₂	S ₂	S ₂	S ₂	S ₁	S ₁	S ₁	S ₁	S ₂	S ₂	
	LS1	0%	0%	0%	0%	0%	0%	0%	0%	0%	0%	0%	0%	0%
LS2	0%	15%	15%	15%	0%	0%	0%	48%	9%	14%	24%	0%	0%	
LS3	99%	82%	82%	82%	95%	99%	99%	51%	90%	84%	76%	96%	99%	
LS4	1%	3%	3%	3%	5%	1%	1%	1%	1%	2%	0%	4%	1%	

6. Conclusions

This study proposes a simulated analytical method to obtain rational fragility functions for 27 Peruvian aerial distribution electrical substations located in Cañete city. Fragility functions allows to estimate seismic vulnerability considering 2000 structural models for each substation. Analyzed models considered variability of structural and seismic parameters.

According to PSHA in Cañete city, a seismic hazard scenario of 0.475g PGA was determined. Projecting this value of fragility curves, seismic vulnerability ratios can be estimated during an earthquake classified as severe, which is related to 475 years of return period and 10% of probability of exceedance. These ratios are not acceptable structural performance levels considering Peruvian seismic code because more than 50 percent



of their seismic vulnerability is located above LS3. This scenario means that the structure is in a pre-collapse state and damages cannot be easily repair. They may require extensive repairing or complete post reposition.

7. References

- [1] Organización Panamericana de la Salud (2010): *Terremoto de Pisco, Perú – A dos años del sismo, crónicas y lecciones aprendidas en el sector salud*. Washington, D.C. USA.
- [2] INDECOPI (2008): *NTP 339.027. HORMIGÓN (CONCRETO). Postes de hormigón (concreto) armado para líneas aéreas*, 8th edición. Perú.
- [3] Luz del Sur S.A.A. (2009): *DNC-098. Postes de concreto para líneas aéreas hasta 22.9 kV (13m)*. Lima. Perú.
- [4] Luz del Sur S.A.A. (2011): *TE-7-533. Plataforma soporte para equipos de peso hasta 1500 kg*. Lima. Perú.
- [5] Luz del Sur S.A.A. (2011): *TE-7-543. Plataforma soporte para equipos de peso hasta 2600 kg*. Lima. Perú.
- [6] Luz del Sur S.A.A. (2008): *TE-7-542. Palomilla doble de concreto armado hasta 250 kVA*. Lima. Perú.
- [7] Luz del Sur S.A.A. (1987): *TE-7-542. Palomilla doble de concreto armado (250), 400 y 630 kVA*. Lima. Perú.
- [8] Luz del Sur S.A.A. (2005): *TE-7-015. Ménsula de concreto armado – 10 kV*. Lima. Perú.
- [9] Luz del Sur S.A.A. (2004): *TE-7-016. Cruceta de concreto armado – 10 kV*. Lima. Perú.
- [10] Luz del Sur S.A.A. (2004): *TE-7-017. Cruceta asimétrica de concreto armado – 10 kV*. Lima. Perú.
- [11] SENCICO, S.N. (2016): *Actualización del programa de Computo Orientado a la Determinación del Peligro Sísmico en el País*. Lima. Perú.
- [12] SENCICO, S.N. (2016): *Actualización del programa de Computo Orientado a la Determinación del Peligro Sísmico en el País, "Manual de Uso del Aplicativo Web"*. Lima. Perú.
- [13] Ministerio de Vivienda, Construcción y Saneamiento - MINSa (2018). *Norma Técnica E.030 "Diseño Sismorresistente"*. Perú.
- [14] Ruiz J (2018): *Estimación de pérdidas por sismos mediante funciones de fragilidad analíticas: caso de dos pabellones universitarios del Cusco. Tesis para optar el grado académico de magíster en ingeniería civil*. PUCP. Lima, Perú.
- [15] Mathworks Inc. (2015): *MATLAB v2015a. The Language of Technical Computing*.
- [16] Moreno R (2006): *Evaluación del riesgo sísmico en edificios mediante análisis estático no lineal: Aplicación a diversos escenarios sísmicos de Barcelona. Tesis para optar el grado académico de doctor en ingeniería civil*. Universidad Politécnica de Cataluña. Barcelona, España.
- [17] Seismosoft (2016): *SeismoArtif. A computer program for generating artificial earthquake accelerograms matched to a specific target response spectrum*.
- [18] Computers and Structures, Inc. (2016): *SAP2000 v.19. Structural Analysis Program*.
- [19] Paulay T and Priestley M (1992): *Seismic design of reinforced concrete and masonry buildings*. John Wiley & Sons. New York, USA.
- [20] Ministerio de Vivienda, Construcción y Saneamiento - MINSa (2009): *Norma Técnica E.060 "Concreto Armado"*. Perú.
- [21] Takeda T, Sozen M. and Nielsen N (1971): *Reinforced concrete response to simulated earthquake*. OHBAYASHI-GUMI, 5. Tokyo, Japón.
- [22] Chunque J (2013): *Nivel de desempeño sísmico del edificio 'A' de la Universidad Privada del Norte. Tesis para optar el título profesional de ingeniero civil*. Universidad Nacional de Cajamarca. Cajamarca, Perú.
- [23] Aguiar R (2003): *Análisis Sísmico por Desempeño*. Universidad de Fuerzas Armadas CEINCI-ESPE. Ecuador.
- [24] Instituto Ecuatoriano de Normalización, INEN (1993): *NTE INEN 1964 (1993) (Spanish): Postes de hormigón armado y preesforzado para soportes de instalaciones de líneas y redes aéreas de energía eléctrica y telecomunicaciones. Definiciones*. Perú.
- [25] Instituto Ecuatoriano de Normalización, INEN (1993): *NTE INEN 1965 (1993) (Spanish): Postes de hormigón armado y preesforzado para soportes de instalaciones de líneas y redes aéreas de energía eléctrica y telecomunicaciones. Requisitos*. Perú.